# Dopaminergic modulation of basal ganglia output through coupled excitation–inhibition

Agata Budzillo[a], Alison Duffy[b], Kimberly E. Miller[c], Adrienne L. Fairhall[d,e,f], and David J. Perkel[c,e,g,1]

[a]Graduate Program in Neurobiology and Behavior, University of Washington, Seattle, WA 98195; [b]Department of Physics, University of Washington, Seattle, WA 98195; [c]Department of Otolaryngology, University of Washington, Seattle, WA 98195; [d]Department of Physiology and Biophysics, University of Washington, Seattle, WA 98195; [e]University of Washington Institute for Neuroengineering, University of Washington, Seattle, WA 98195; [f]Center for Sensorimotor Neural Engineering, University of Washington, Seattle, WA 98195; and [g]Department of Biology, University of Washington, Seattle, WA 98195

Edited by Terrence J. Sejnowski, Salk Institute for Biological Studies, La Jolla, CA, and approved April 14, 2017 (received for review July 18, 2016)

**Learning and maintenance of skilled movements require exploration of motor space and selection of appropriate actions. Vocal learning and social context-dependent plasticity in songbirds depend on a basal ganglia circuit, which actively generates vocal variability. Dopamine in the basal ganglia reduces trial-to-trial neural variability when the bird engages in courtship song. Here, we present evidence for a unique, tonically active, excitatory interneuron in the songbird basal ganglia that makes strong synaptic connections onto output pallidal neurons, often linked in time with inhibitory events. Dopamine receptor activity modulates the coupling of these excitatory and inhibitory events in vitro, which results in a dynamic change in the synchrony of a modeled population of basal ganglia output neurons receiving excitatory and inhibitory inputs. The excitatory interneuron thus serves as one biophysical mechanism for the introduction or modulation of neural variability in this circuit.**

songbird | learning | variability | basal ganglia | dopamine

The basal ganglia are implicated in the acquisition, initiation, and selection of motor acts (1, 2). Striatal dopamine plays a critical role in regulating these processes (3–5), but little is known about how dopamine modulates basal ganglia microcircuitry to change behavior.

Song, used by male songbirds for territory defense and mate selection, is learned through trial and error. Songbirds possess discrete forebrain nuclei whose roles in song learning and production have been partially mapped (Fig. 1*A*) (6). Due to this relatively well-characterized functional anatomy, the birdsong learning circuit has been a rich testing ground for the development of biologically plausible models of skill learning (7–10). The model of reinforcement learning establishes an important role for variability in learning. Although, following crystallization, adult song is a highly stereotyped motor behavior, it is affected by social context: courtship song is considerably less variable than song produced in isolation (11). This ongoing variability could support song maintenance or adult learning (12–15). Songbirds thus pose a unique opportunity to determine the circuit mechanisms underlying context-dependent switching and the role of variability in a learned social behavior.

A basal ganglia loop is essential for song learning (16, 17). Area X is the basal ganglia structure of the song system; it contains many spiny neurons (Fig. 1*B*) and fewer pallidal output neurons (18). One of its roles is to regulate song variability (Fig. 1*C*) (19). Although variability reaches the motor pathway through the cortex-like output area lateral magnocellular nucleus of the anterior nidopallium (LMAN) (20, 21), its exact source and the mechanism for its generation are unknown. Area X transforms stereotyped inputs from the premotor, cortex-like nucleus HVC (proper name) (22) into variable firing of its output neurons (23); this transformation could contribute to modulating vocal variability. During courtship, when birds sing directed song, dopaminergic neurons in the midbrain, homologous to those carrying reward signals in mammals (24–26), increase dopamine levels in area X (27). This increased dopamine acts through D1 receptors to reduce vocal variability (28).

How could dopamine affect the microcircuitry of area X to modulate variability? Time-locked inputs from HVC (29) drive very similar firing patterns in area X spiny neurons independent of social context (23, 29, 30). Spiny neurons inhibit the pallidal output neurons, which, in contrast, show changes in firing variability with social context (Fig. 1*C*) (23, 31–34). The mechanism underlying this transformation in area X, which could contribute to modulating firing variability in downstream nuclei, is not understood.

To determine how dopamine influences the circuit properties within area X to shape the firing properties of its output, we recorded intracellularly from area X pallidal neurons in brain slices, focusing on their synaptic inputs. We report a unique, local, spontaneously active glutamatergic neuron type, which shifts the circuitry of this basal ganglia nucleus from strictly inhibitory to mixed inhibitory–excitatory. This excitatory component of area X contributes to variability in pallidal neuron firing. Such an excitatory component could serve as a functional analog of subthalamic nucleus input, which is lacking in area X. A simple model suggests a powerful mechanism for dopaminergic modulation. We propose a unique microcircuit switch that could allow dopamine to control the variability and synchrony of the pallidal population and in turn to shape motor output according to social context.

## Results

**Rhythmic Excitatory Inputs to Pallidal Neurons.** We visually targeted pallidal neurons for recording in isolated area X brain slices. They showed regular, spontaneous firing at nearly 60 Hz [mean interspike interval (ISI) of 17.3; SD = 13.8 ms; mean coefficient of variation (CV) of ISI of 0.19; SD = 0.15; $n = 153$, Fig. 1*D* and Fig. S1]. We hypothesized that synaptic potentials contributed to the spread in the ISI distribution. Injecting hyperpolarizing current to block spontaneous firing revealed substantial spontaneous synaptic

### Significance

Trial-and-error learning requires variation in successive trials, but the source of such variability is unknown. We describe a unique striatal glutamatergic neuron in the zebra finch. This neuron exerts a potent, dopamine-regulated action on pallidal output neurons that modifies neuronal firing statistics in the circuit known to contribute to vocal variability. A simple model reveals how this microcircuit could be influenced by social context and striatal dopamine to switch between firing patterns that modify song variability essential for vocal learning.

Author contributions: A.B., A.D., A.L.F., and D.J.P. designed research; A.B., A.D., A.L.F., and K.E.M. performed research; A.B., A.D., K.E.M., and D.J.P. analyzed data; and A.B., A.D., and D.J.P. wrote the paper.

The authors declare no conflict of interest.

This article is a PNAS Direct Submission.

[1]To whom correspondence should be addressed. Email: perkel@uw.edu.

This article contains supporting information online at www.pnas.org/lookup/suppl/doi:10.1073/pnas.1611146114/-/DCSupplemental.

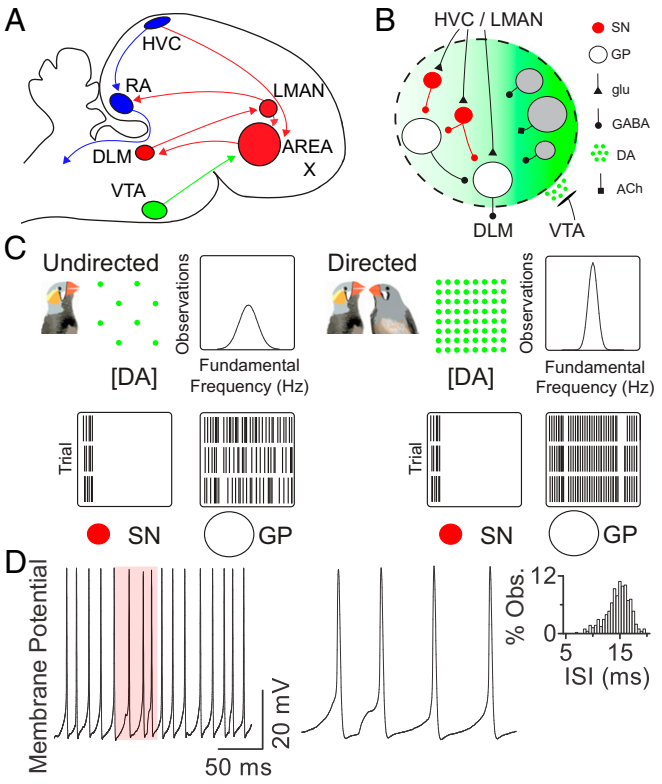


**Fig. 1.** Effects of social context and dopamine on area X neuron firing. (*A*) Diagram of the songbird brain. Blue, motor pathway; red, learning pathway; green, midbrain dopamine input. (*B*) Circuitry within area X. Red, spiny neurons (SN); gray; local interneurons; white, pallidal neurons (GP). ACh, acetylcholine; DA, dopamine; glu, glutamate. (*C*) Schematic of social context-dependent changes in behavior and neural activity in area X (after refs. 20 and 23). During courtship, area X DA rises, narrowing the distribution of fundamental frequency across song trials. Simultaneously, area X GP output neuron firing becomes less variable. Input SNs maintain precise firing. (*D*) Regular pallidal neuron firing. (*Left*) Example pallidal neuron recording in current-clamp configuration with no current injection. (*Center*) Magnification of shaded region at *Left* illustrates underlying synaptic potentials. (*Right*) Interspike interval (ISI) distribution for this neuron.

activity (Fig. 2*A*). Many events were inhibitory, consistent with the overwhelming dominance of GABAergic neurons in basal ganglia (18, 32, 34–37). Surprisingly, however, many synaptic events were excitatory. Excitatory postsynaptic potentials (EPSPs) tended to occur at regular intervals, and 23.1% (SD = 19.1%; $n = 31$) were closely followed by inhibitory postsynaptic potentials (IPSPs) (Fig. 2*A*, asterisks).

Voltage-clamp recordings revealed prominent glutamatergic excitatory postsynaptic currents (EPSCs) and GABAergic inhibitory postsynaptic currents (IPSCs) in all pallidal neurons. EPSCs were blocked by glutamate receptor blockers 2,3-dioxo-6-nitro-1,2,3,4-tetrahydrobenzo[*f*]quinoxaline-7-sulfonamide (NBQX) and D, L-aminophosphonovalerate (APV) (Fig. 2*B*). IPSCs were blocked by the $GABA_A$ receptor antagonist gabazine (Fig. 2*C*). As in current-clamp mode, EPSCs were frequently followed by IPSCs (Fig. 2 *B* and *C*, asterisks). Expanded views of such EPSCs followed by IPSCs, which we termed "linked events," are shown in Fig. 2*D*.

These excitatory inputs likely arise within area X, because EPSCs were present when area X was removed from surrounding tissue, depended on action potentials, and slowed with application of the $GABA_A$ receptor agonist muscimol (Fig. S2). EPSCs were regular; the inter-EPSC interval mode averaged 48.6 ± 17.5 ms (Fig. 2*E*). Together, these results show that a glutamatergic neuron in area X firing at ∼20 Hz excites pallidal neurons. Such EPSCs were not seen in 15 spiny neurons (data from this study and ref. 38).

The spontaneous EPSCs can influence pallidal neuron firing. EPSCs were often large (mean amplitude, 64.18 ± 31.02 pA; $n = 32$) and could exceed 100 pA (Fig. 2*F*). They had a fast, smooth rising phase (Fig. 2*G*), consistent with a unitary input arising from a single presynaptic neuron. These EPSCs are thus able to deliver potent excitation to pallidal neurons, as we saw in current-clamp mode, where EPSPs were frequently on the order of 3–5 mV (Fig. 2*A*). In a few cases, we recorded simultaneously from two nearby pallidal neurons and observed many coincident EPSCs, suggesting that the putative excitatory neuron is divergent, simultaneously driving a population of pallidal output cells (Fig. 2*H*).

Previous unpublished work suggested that a population of area X neurons express VGluT2 mRNA (ZEBrA database; Oregon

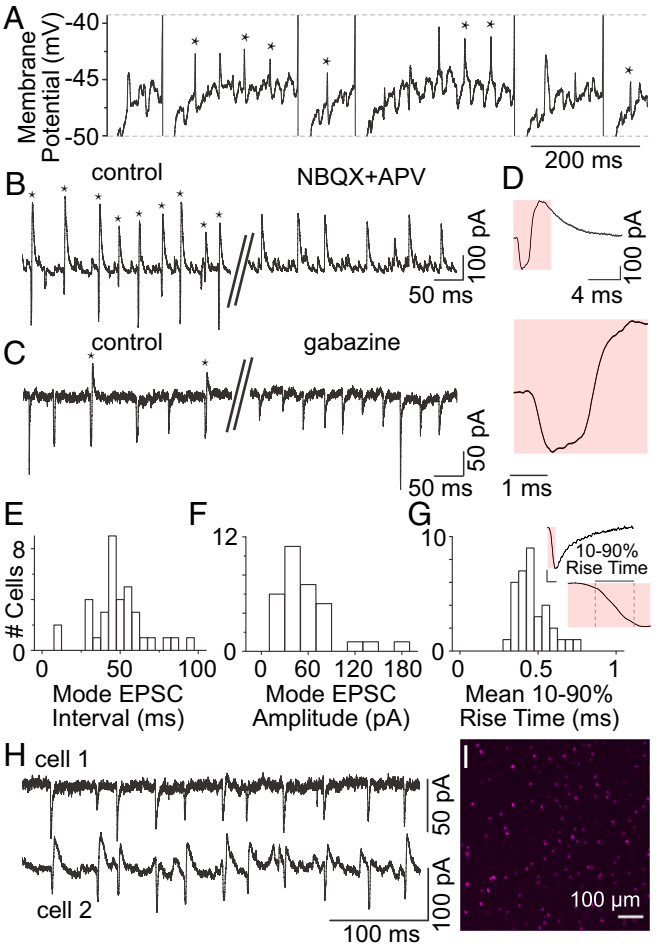


**Fig. 2.** Large, regular, unitary glutamatergic synaptic events impinge on area X pallidal neurons. (*A*) Current-clamp recording showing large regular EPSPs (asterisks) observed during steady injection of hyperpolarizing current. Dashed lines indicate truncated action potentials. (*B*) In voltage-clamp mode, EPSCs were often observed linked with IPSCs (asterisks). EPSCs were blocked by the AMPA receptor antagonist NBQX. (*C*) IPSCs were blocked by the $GABA_A$ receptor antagonist gabazine. (*D*) Expanded views of a linked EPSC/IPSC event. (*E*) Inter-EPSC interval mode across 36 neurons, indicating a rate of ∼20 Hz. (*F*) EPSC amplitude mode across 32 neurons, indicating strong excitatory inputs to pallidal cells. (*G*) EPSCs had fast rise times (mean rise time, 0.47 ± 0.10 ms; $n = 35$ neurons), consistent with a unitary origin. (*H*) Example paired recording showing that two pallidal cells receive simultaneous EPSCs. The most likely explanation is that they arise from a single presynaptic excitatory neuron. (*I*) Low-power in situ hybridization showing sparse cells expressing mRNA for vGluT2 in area X (magenta).

Health and Science University; www.zebrafinchatlas.org). We confirmed this finding (Fig. 2*I* and Fig. S3*B*) and found that, unlike in mammals (39, 40), area X cholinergic interneurons are not glutamatergic (Fig. S3 *A–D*). We found that some vGluT2$^+$ neurons in area X also express mRNA for glutamic acid decarboxylase 1 (GAD1), a marker for GABAergic neurons (Figs. S4 and S5), although some vGluT2 neurons do not appear to be GABAergic (Figs. S5 and S6).

**Two Distinct Microcircuit Configurations Modulated by Dopamine.** These strong inputs influence pallidal firing variability. Blocking AMPA glutamate receptors with NBQX decreased the variability of spontaneous pallidal neuron firing without changing the overall firing rate (Fig. 3 *A–C*).

The D1 receptor agonist SKF-38393 did not alter the overall frequency of EPSCs or IPSCs; rather, it increased the proportion of coupled events (Fig. 3 *D–F*). It also increased the absolute rate of coupled events (Fig. S7). The modulation of these coupled events by dopamine represents a mechanism for altering the configuration of area X microcircuitry.

Given the divergence of the excitatory input, we considered the microcircuit motif defined by this neuron, its coupled inhibitory partner, and the population of pallidal neurons that they drive. We explored how switching the microcircuit from isolated to coupled EPSCs and IPSCs (Fig. 3 *E* and *F*) might contribute to dopaminergic modulation of pallidal neuron firing variability during courtship singing. We used a simple model of a pallidal neuron with experimentally determined phase response curves (PRCs) to predict how its firing regularity was affected by excitatory inputs alone or excitatory and inhibitory inputs together. We explored the robustness of this behavior to changes in multiple parameters, and to the observed dopamine-driven increase in coupled synaptic inputs. This model also allowed us to evaluate the firing properties of a population of pallidal neurons receiving the same microcircuit synaptic inputs.

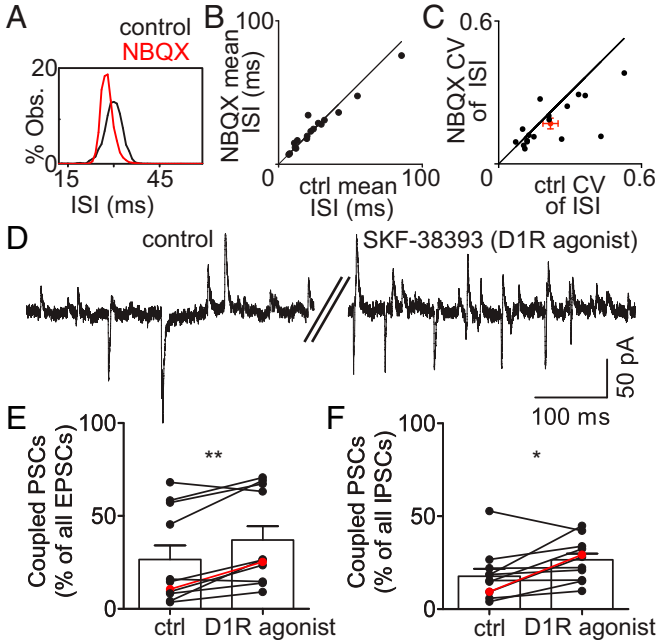


**Fig. 3.** EPSCs introduce variability into pallidal neuron firing and are modulated by DA. (*A*) ISI distribution for one example neuron before and after application of 10 μM NBQX, illustrating reduction in ISI variability. (*B*) Scatter plot of mean ISI; 10 μM NBQX did not change mean ISI (control, 25.9 ± 4.81 ms, vs. NBQX, 25.6 ± 4.12 ms; $P = 0.78$; $n = 17$ neurons). (*C*) NBQX significantly decreased variability of pallidal firing (control CV, 0.22 ± 0.03, vs. NBQX CV, 0.17 ± 0.02; $P = 0.045$). Error bars represent SEM. (*D*) The D1 dopamine receptor agonist SKF-38393 increased the incidence of linked synaptic events. (*E* and *F*) Summary data for $n = 11$ pallidal neurons in 10 μM SKF-38393. Example in *D* is indicated in red. (*E*) D1R agonist significantly increased the percentage of all EPSCs that led an IPSC by at most 4 ms (control, 26.7 ± 7.51 ms, vs. D1R agonist, 37.1 ± 7.46 ms; $P = 0.003$; mean of differences, −10.4; 95% CI, −16.3 to −4.48). (*F*) D1R agonist significantly increased the percentage of all IPSCs that are preceded by an EPSC within 4 ms (control, 17.8 ± 4.06 ms, vs. D1R agonist, 26.6 ± 3.38 ms; $P = 0.024$; mean of differences, −8.85; 95% CI, −16.2 to −1.47). Error bars represent SEM. $*P \leq 0.05$ and $**P \leq 0.01$.

We modeled the intrinsically, regularly firing pallidal neurons using a model whose only state variable is phase (41). The experimentally measured infinitesimal PRC (iPRC), which describes the shift in phase on the next spike as a function of the phase at which a perturbation is provided, allowed realistic modeling of the interaction between oscillating neuron types (Fig. 4 *A–C*) (42). We fit EPSC and coupled EPSC–IPSC waveforms (Fig. 4 *D* and *E*) and convolved them with the iPRC. See Table S1 for fit parameters. The resulting "microcircuit PRCs" capture the effect of each input type on pallidal neuron spike timing (43). We then built firing maps relating the pallidal phase of the arrival of one synaptic input to that of the next synaptic input (44, 45) (rightmost panels of Fig. 4 *D* and *E*). We determined the model response to ongoing, periodic input of either EPSCs alone or coupled EPSC–IPSC events, to simulate the effect of dopamine (Fig. 4 *F* and *G*). We found that EPSCs alone could cause cycle-to-cycle changes to the pallidal phase at which synaptic input arrives, implying irregular pallidal neuron firing. We can model a population of desynchronized pallidal neurons or a single neuron on different trials by initializing the simulation at different initial phases. This led to a broad phase distribution (Fig. 4*F*, *Right*, blue curve). In contrast, with coupled EPSC–IPSC events, regardless of initial phase, the phase distribution collapsed to a single value, implying both regular pallidal neuron firing (Fig. 4*G*, *Right*) and population-level synchrony. Such a transition could also occur if synaptic inputs became coupled during a trial (Fig. 4*H*).

This switch between regular and irregular firing occurred over a large range of realistic input parameter settings (Fig. 5 *A* and *B*). We varied the strength and period of the synaptic input relative to the pallidal neuron firing period. We measured firing variability by computing the entropy, a measure of the width of the phase probability distribution (45). Large areas of parameter space showed stark differences in entropy under the two microcircuit configurations (Fig. 5 *A* and *B*), indicating that the observed synaptic changes caused by dopamine could cause a change in firing variability and synchrony.

Because our experiments showed that excitatory events couple to inhibitory events in a probabilistic manner, we explored smoothly changing the probability of isolated and coupled events. We found that changes in the probability of coupled events on the order of those recorded experimentally (dopamine receptor activation increased the fraction of coupled synaptic events in most neurons by between approximately 0 and +200%) could cause substantial changes in the entropy of the phase–probability distribution (Fig. 5*C*). Together, our simulation results show that a simple and highly constrained model microcircuit of area X can explain the observed effects of dopamine on variability of pallidal neuron firing. Small dopamine-induced shifts in the prevalence of coupled synaptic events could thus provide a continuous adjustment to the degree of pallidal neuron firing variability and population synchrony.

## Discussion

Our main findings are as follows: a regularly firing excitatory neuron type located within area X makes strong synaptic connections to multiple area X output neurons; this excitatory input is temporally tightly coupled to inhibitory input; it contributes to

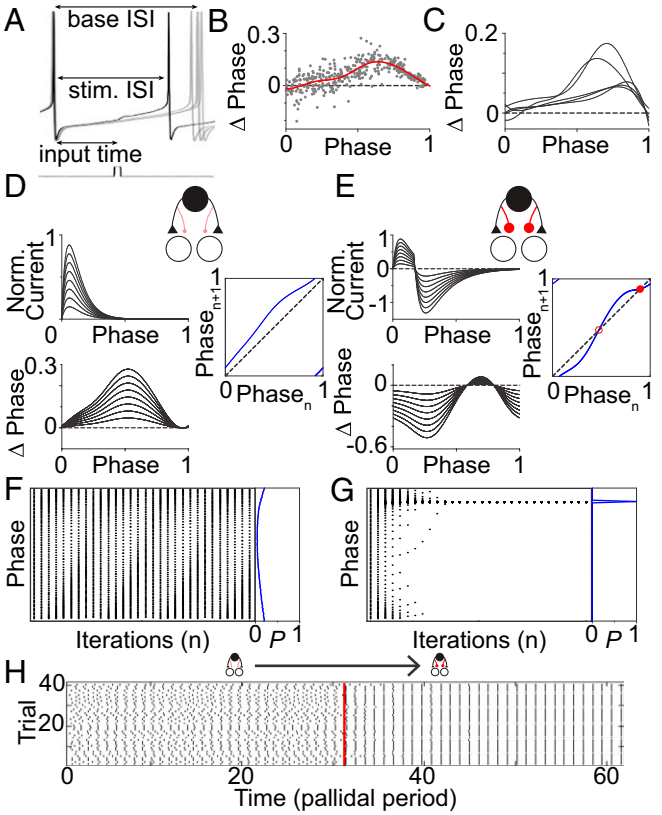


**Fig. 4.** Experimentally measured pallidal iPRC constrains simple model of how DA affects the area X microcircuit. (*A*) Example of pallidal phase shifts caused by small current pulse (50 pA, 2 ms). (*B*) Phase shifts caused by single current pulses in a pallidal neuron. Red curve represents analytic fit to those points ($R^2 = 0.52$). (*C*) Individual fits to five pallidal neurons show qualitative similarity. (*D*) We convolved the normalized EPSC (*Upper Left*) with the parameterized iPRC (*C*) to obtain the microcircuit PRC (*Lower Left*). Multiple synaptic strengths are shown. (*Right*) Firing map iteratively relating the phase of the pallidal neuron at the onset of one input to its phase at the time of the next input. (*E*) Same as in *D* but for linked excitatory–inhibitory (EI) synaptic events. Filled red circle in firing map indicates a stable fixed point; open red circle indicates unstable fixed point. (*F*) Trajectory of the firing phases of pallidal neuron ensemble relative to excitatory neuron under excitatory (E) microcircuit drive. (*Left*) Pallidal phase ensemble evolution under firing map drive across multiple initial conditions (Fig. 4*D*). (*Right*) Blue line plots the resulting phase probability distribution. Note lack of convergence to a single phase (high entropy, low synchrony). (*G*) Same as in *F* for EI microcircuit drive. Note convergence of pallidal ensemble to a single phase (low entropy, high synchrony). (*H*) Change in firing of pallidal ensemble over time as microcircuit shifts from excitation only to mixed excitation and inhibition. Each dot represents a pallidal neuron firing event, and each row indicates the progression of a single trial with a different, randomly selected initial phase. Vertical red line indicates the time when the microcircuit switched.

pallidal firing variability and potentially the synchrony of output subpopulations; and these inputs are modulated by dopamine. Such synaptic inputs drive irregular firing in simple model output neurons, as during variable singing when a bird is alone. Dopamine-induced changes shift a modeled population of pallidal neurons from irregular to regular firing, or from asynchrony to synchrony. Such context-dependent changes in circuit dynamics are well placed to modulate behavioral variability to drive learning.

We have provided evidence for a unique glutamatergic excitatory basal ganglia neuron type. A subset of these neurons may corelease GABA. It is not the cholinergic neuron type, which also releases glutamate in mammals (40, 46), but may nonetheless have similar function. In mammals, neurons of the subthalamic nucleus (STN) fire rhythmically and excite pallidal output neurons (47). Loss of dopamine, as occurs in Parkinson's disease, leads to inappropriately synchronized and oscillatory firing of STN and pallidal neurons. The avian STN homolog (48) is not connected to area X (31). Local glutamatergic activity in area X may thus be functionally analogous to that provided by the STN; perhaps packaging these neurons within the nucleus allows for fine temporal precision, as required for song.

The unique glutamatergic cell type is likely rare, as it has not been recorded previously (18) and it appears to be relatively sparse (Fig. 2*I*). However, the ubiquity and potency of spontaneous EPSCs in pallidal neurons suggests that the glutamatergic neuron exerts widespread impact on its postsynaptic targets, consistent with simultaneous EPSCs in pairs of pallidal neurons.

Our modeling suggests that the frequent coupling of EPSCs and IPSCs is an important feature of the circuitry in area X. Changing model parameters according to observed effects of dopamine could easily switch the circuit into a regime of low pallidal firing variability. This variability may be key for creating firing pauses whose timing can drive activity in the medial portion of the dorsolateral nucleus of the anterior thalamus (DLM) (49–51). The precise source of coupling is not entirely clear, yet its persistence after glutamate blockade argues against a

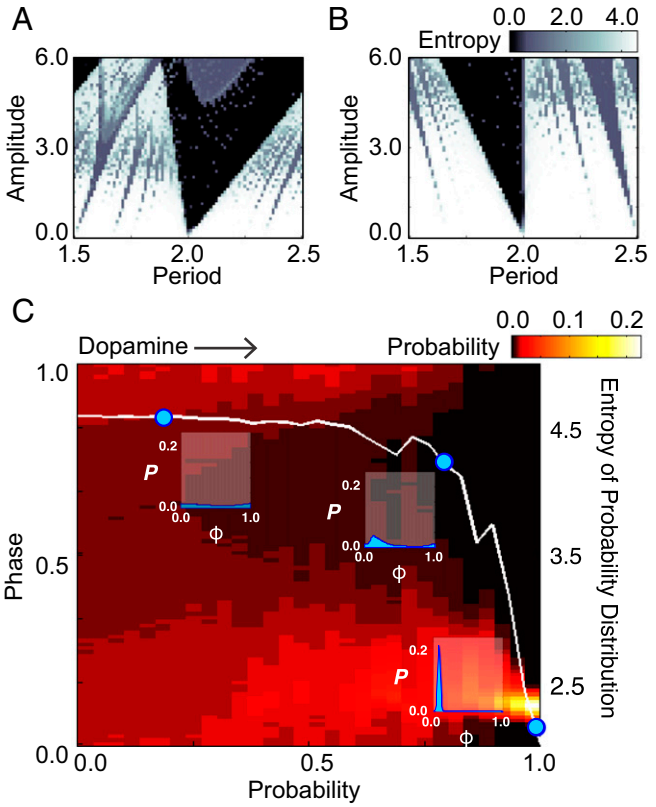


**Fig. 5.** Neural firing entropy from a simple model of the area X microcircuit in different conditions. (*A*) The entropy of the distribution of pallidal firing phase varies with synaptic amplitude and period of E microcircuit drive relative to pallidal period. (*B*) Same as *A*, but for EI microcircuit. (*C*) Effects of probabilistic inclusion of the inhibitory element on firing-phase distribution. Pallidal neuron intrinsic firing had low variability (CV = 0.05). Heat map shows the effect on the pallidal phase–probability distribution as the probability of selecting the EI microcircuit varied from 0 to 1 (abscissa). For each EI probability, the resulting phase (left ordinate) probability distribution is plotted as a column of heat values. Entropy from each column is plotted (right ordinate) as a white line. *Insets* show the probability distribution at three example EI probability values, corresponding to blue circles.

glutamate-driven disynaptic origin. Although we found some neurons coexpressing glutamatergic and GABAergic markers, the variable timing of the IPSC relative to the EPSC (Fig. S6) argues against corelease of glutamate and GABA as the main mechanism for coupling the events (52–57). A possible alternative mechanism is gap-junction coupling between the glutamatergic and GABAergic neurons.

Although we have shown one way in which area X may contribute to or regulate variability in the song learning circuit, variability is often attributed to nucleus LMAN (12, 19, 58, 59). Area X can exert a strong, precisely timed influence on LMAN via DLM (50, 51, 60, 61). A change between synchronous and asynchronous activity in the area X pallidal population could affect its ability to propagate signals through DLM, allowing basal ganglia to temporally modulate variability generated within LMAN. Area X projections to DLM neurons are thought to be one-to-one, but ensembles of DLM neurons converge on LMAN neurons (62–64), allowing area X to have a potentially dramatic effect on LMAN firing. Furthermore, these inputs preserve a myotopic organization of connectivity that runs throughout the learning circuit to the output motor drive (65–67). Momentary coherence of multiple area X pallidal neurons could thus control the activity of coordinated downstream neuron groups. The DLM input could cause recurrent networks such as those within LMAN to undergo stimulus-dependent suppression of their intrinsic, potentially chaotic activity (68). Indeed, highly correlated firing of neurons in HVC and in LMAN, presumably sustained through the polysynaptic basal ganglia loop, suggests a high degree of synchronous firing among local neuronal populations, perhaps within area X (69). Temporal variations in area X dopamine could not only create social context-dependent changes in variability but could also generate precisely timed shifts in variability that are presumably required for the ability of adult birds to learn to produce changes in specific song syllables (69, 70). Temporarily pooling specific subsets of area X output neurons could therefore act to create temporally precise, task-specific signals.

Glutamatergic neurons intrinsic to area X are thus well placed to contribute to the rapid changes in network dynamics induced by different social and learning contexts. Furthermore, they fire in microcircuit motifs that can strongly influence their downstream impact. Dopamine modulation of these coupled synaptic events provides a unique biophysical mechanism for rapidly switching area X firing patterns. Our model predicts that dopamine acts on the glutamatergic neuron type to orchestrate a transition between a regime of asynchronous and/or variable firing to one of synchronous and/or less variable firing. Silencing the excitatory neuron should then disrupt context-dependent transitions in pallidal neuron synchrony and perhaps also vocal variability. These predictions remain to be tested through simultaneous recordings from multiple pallidal neurons in vitro and in vivo.

We propose a specific biophysical mechanism contributing to modulating behavioral variability that is important for learning precise skilled movements. Similar mechanisms could underlie action selection, a hypothesized function of the basal ganglia (2, 71). Loss of dopamine, as in Parkinson's disease, results in synchronous pallidal firing and more variable movement dynamics. More broadly, outside the motor domain, neural variability could give rise to adaptive phenomena such as effective foraging or creativity, or to maladaptive phenomena such as intrusive thoughts or attention deficit hyperactivity disorder (ADHD). Just as the presence of a female songbird raises striatal dopamine in the male and increases song stereotypy, stimulants acting through dopamine receptors reduce impulsive behaviors and enhance mental focus in patients with ADHD. The readily quantified song behavior and its discrete underlying neural circuit offer a promising pathway for detailed mechanistic analysis of basal ganglia function in health and disease.

## Materials and Methods

**Electrophysiology.** The 250-μm parasagittal brain slices were collected from 40 adult male zebra finches as in ref. 18. We cut around area X in each slice, thereby removing the cell bodies of projections to area X. Recordings from isolated area X slices were performed in artificial cerebrospinal fluid (ACSF) at 30 °C with high-chloride intracellular solution. See *Supporting Information* for detailed methods and data-inclusion criteria. The following drugs were bath applied: NBQX, muscimol, SKF-38393 hydrobromide, DL-APV (Tocris); gabazine/SR-95531 (Sigma-Aldrich); TTX (Calbiochem).

**iPRC Measurement.** iPRC experiments were conducted following ref. 42 (*Supporting Information*). The 2-ms current pulses were injected at a frequency of 2 Hz, with four stimulus presentations per sweep, and repeated at different amplitudes (±50/100/250 pA). Phase change was defined as the difference between the baseline ISI and the stimulated ISI divided by the mean baseline ISI. The experimental iPRC was fit to an analytical form.

**Firing Map Construction.** The $PRC_{syn}$ was calculated by convolving the iPRC with either an excitatory synaptic input (E) or a coupled excitatory–inhibitory input (EI). Synaptic waveforms for E and EI inputs were drawn directly from fits to the two classes of synaptic input observed in our data (*Supporting Information*). We constructed the firing map as follows:

$$\phi_{n+1} = \{\phi_n + PRC_{syn}(\phi_n) + T_{mc}\}_{mod\ T_p},$$

where $T_{mc}$ is the period of the microcircuit inputs and $T_p$ is the period of the pallidal cell. $\phi_n$ is the pallidal phase at which the $n$th synaptic input arrives.

**Calculation of Entropy.** We calculated the entropy of phase distributions by approximating the steady state probability density function of a cell ensemble. Phase (0–1) was discretized, and a probability mass function was estimated by normalizing the counts of cells in each phase bin. Entropy was defined as follows:

$$S = -\sum_{i=1}^{M} p(\varphi_i)\ln(p(\varphi_i)).$$

**Modeling of Noise in ISI Distribution and Likelihood of E–I vs. E Microcircuit.** We consider two aspects of noise: $\eta$ models variability in the pallidal ISI as a Gaussian random variable; we model probabilistic jumps between microcircuit states as Bernoulli draws of firing maps $f$ and $g$, the firing maps of the respective E and EI microcircuit drives. The probability of either the E or EI microcircuit occurring at any one input is as follows:

$$P\{\phi_{n+1} = f(\phi_n)\} = 1 - P\{\phi_{n+1} = g(\phi_n)\}.$$

Results in Fig. 5C were computed by varying the Bernoulli probability of the EI firing map on a single draw from zero to 1.

**Statistics.** Calculations are specified as mean ± SD or SEM. ISI variability was quantified using the CV (CV = SD/mean). Synaptic events before and after applications of NBQX, APV, TTX, muscimol, and SKF-38393 were quantified with paired two-tailed $t$ tests. Coupled events were quantified by the percentage of all synaptic events of the relevant type (EPSC or IPSC). Traces and summary data depicted in figures are available from the corresponding author upon request.

**ACKNOWLEDGMENTS.** We thank Dr. Pankaj Sah for suggesting the analysis of EPSC-IPSC relative timing as shown in Fig. S6. This work was funded by NIH Grant R01MH066128 (to D.J.P.) and National Science Foundation Award IIS 1421245 (to A.L.F.). A.D. was also funded through NIH Training Grant 1T90DA032436, and A.B. through Grants T32DC000033 and T32GM007108. A.L.F. acknowledges the support of the Washington Research Foundation.

1. Graybiel AM (2005) The basal ganglia: Learning new tricks and loving it. *Curr Opin Neurobiol* 15:638–644.
2. Graybiel AM, Grafton ST (2015) The striatum: Where skills and habits meet. *Cold Spring Harb Perspect Biol* 7:a021691.
3. Bromberg-Martin ES, Matsumoto M, Hikosaka O (2010) Dopamine in motivational control: Rewarding, aversive, and alerting. *Neuron* 68:815–834.
4. Schultz W (2013) Updating dopamine reward signals. *Curr Opin Neurobiol* 23:229–238.

5. Wise RA (2009) Roles for nigrostriatal—not just mesocorticolimbic—dopamine in reward and addiction. *Trends Neurosci* 32:517–524.
6. Fee MS, Scharff C (2010) The songbird as a model for the generation and learning of complex sequential behaviors. *ILAR J* 51:362–377.
7. Doya K, Sejnowski TJ (1998) A computational model of birdsong learning by auditory experience and auditory feedback. *Central Auditory Processing and Neural Modeling*, eds Poon P, Brugge J (Plenum, New York), pp 77–88.
8. Rao RP, Sejnowski TJ (2001) Spike-timing-dependent Hebbian plasticity as temporal difference learning. *Neural Comput* 13:2221–2237.
9. Farries MA, Fairhall AL (2007) Reinforcement learning with modulated spike timing dependent synaptic plasticity. *J Neurophysiol* 98:3648–3665.
10. Fiete IR, Fee MS, Seung HS (2007) Model of birdsong learning based on gradient estimation by dynamic perturbation of neural conductances. *J Neurophysiol* 98: 2038–2057.
11. Sossinka R, Böhner J (1980) Song types in the zebra finch *Poephila guttata castanotis*. *Z Tierpsychol* 53:123–132.
12. Ali F, et al. (2013) The basal ganglia is necessary for learning spectral, but not temporal, features of birdsong. *Neuron* 80:494–506.
13. Andalman AS, Fee MS (2009) A basal ganglia-forebrain circuit in the songbird biases motor output to avoid vocal errors. *Proc Natl Acad Sci USA* 106:12518–12523.
14. Sakata JT, Brainard MS (2008) Online contributions of auditory feedback to neural activity in avian song control circuitry. *J Neurosci* 28:11378–11390.
15. Tumer EC, Brainard MS (2007) Performance variability enables adaptive plasticity of "crystallized" adult birdsong. *Nature* 450:1240–1244.
16. Bottjer SW, Miesner EA, Arnold AP (1984) Forebrain lesions disrupt development but not maintenance of song in passerine birds. *Science* 224:901–903.
17. Scharff C, Nottebohm F (1991) A comparative study of the behavioral deficits following lesions of various parts of the zebra finch song system: Implications for vocal learning. *J Neurosci* 11:2896–2913.
18. Farries MA, Perkel DJ (2002) A telencephalic nucleus essential for song learning contains neurons with physiological characteristics of both striatum and globus pallidus. *J Neurosci* 22:3776–3787.
19. Kao MH, Doupe AJ, Brainard MS (2005) Contributions of an avian basal ganglia-forebrain circuit to real-time modulation of song. *Nature* 433:638–643.
20. Kao MH, Brainard MS (2006) Lesions of an avian basal ganglia circuit prevent context-dependent changes to song variability. *J Neurophysiol* 96:1441–1455.
21. Olveczky BP, Andalman AS, Fee MS (2005) Vocal experimentation in the juvenile songbird requires a basal ganglia circuit. *PLoS Biol* 3:e153.
22. Reiner A, et al.; Avian Brain Nomenclature Forum (2004) Revised nomenclature for avian telencephalon and some related brainstem nuclei. *J Comp Neurol* 473:377–414.
23. Woolley SC, Rajan R, Joshua M, Doupe AJ (2014) Emergence of context-dependent variability across a basal ganglia network. *Neuron* 82:208–223.
24. Bottjer SW (1993) The distribution of tyrosine hydroxylase immunoreactivity in the brains of male and female zebra finches. *J Neurobiol* 24:51–69.
25. Lewis JW, Ryan SM, Arnold AP, Butcher LL (1981) Evidence for a catecholaminergic projection to area X in the zebra finch. *J Comp Neurol* 196:347–354.
26. Gerfen CR, Surmeier DJ (2011) Modulation of striatal projection systems by dopamine. *Annu Rev Neurosci* 34:441–466.
27. Sasaki A, Sotnikova TD, Gainetdinov RR, Jarvis ED (2006) Social context-dependent singing-regulated dopamine. *J Neurosci* 26:9010–9014.
28. Leblois A, Wendel BJ, Perkel DJ (2010) Striatal dopamine modulates basal ganglia output and regulates social context-dependent behavioral variability through D1 receptors. *J Neurosci* 30:5730–5743.
29. Hahnloser RHR, Kozhevnikov AA, Fee MS (2002) An ultra-sparse code underlies the generation of neural sequences in a songbird. *Nature* 419:65–70.
30. Kozhevnikov AA, Fee MS (2007) Singing-related activity of identified HVC neurons in the zebra finch. *J Neurophysiol* 97:4271–4283.
31. Person AL, Gale SD, Farries MA, Perkel DJ (2008) Organization of the songbird basal ganglia, including area X. *J Comp Neurol* 508:840–866.
32. Carrillo GD, Doupe AJ (2004) Is the songbird area X striatal, pallidal, or both? An anatomical study. *J Comp Neurol* 473:415–437.
33. Farries MA, Ding L, Perkel DJ (2005) Evidence for "direct" and "indirect" pathways through the song system basal ganglia. *J Comp Neurol* 484:93–104.
34. Reiner A, Laverghetta AV, Meade CA, Cuthbertson SL, Bottjer SW (2004) An immunohistochemical and pathway tracing study of the striatopallidal organization of area X in the male zebra finch. *J Comp Neurol* 469:239–261.
35. Gittis AH, Kreitzer AC (2012) Striatal microcircuitry and movement disorders. *Trends Neurosci* 35:557–564.
36. Luo M, Perkel DJ (1999) A GABAergic, strongly inhibitory projection to a thalamic nucleus in the zebra finch song system. *J Neurosci* 19:6700–6711.
37. Luo M, Perkel DJ (1999) Long-range GABAergic projection in a circuit essential for vocal learning. *J Comp Neurol* 403:68–84.
38. Thompson JA, Perkel DJ (2011) Endocannabinoids mediate synaptic plasticity at glutamatergic synapses on spiny neurons within a basal ganglia nucleus necessary for song learning. *J Neurophysiol* 105:1159–1169.
39. Guzman MS, et al. (2011) Elimination of the vesicular acetylcholine transporter in the striatum reveals regulation of behaviour by cholinergic-glutamatergic co-transmission. *PLoS Biol* 9:e1001194.
40. Higley MJ, et al. (2011) Cholinergic interneurons mediate fast VGluT3-dependent glutamatergic transmission in the striatum. *PLoS One* 6:e19155.
41. Ermentrout GB, Kopell N (1986) Parabolic bursting in an excitable system coupled with a slow oscillation. *SIAM J Appl Math* 46:233–253.
42. Farries MA, Wilson CJ (2012) Phase response curves of subthalamic neurons measured with synaptic input and current injection. *J Neurophysiol* 108:1822–1837.
43. Netoff T, Schwemmer M, Lewis T (2012) Experimentally estimating phase response curves of neurons: Theoretical and practical issues. *Phase Response Curves in Neuroscience: Theory, Experiment, and Analysis*. Springer Series in Computational Neuroscience, eds Schultheiss NW, Prinz AA, Butera RJ (Springer Science & Business Media, New York), Vol 6, pp 95–129.
44. Izhikevich EM (2007) *Dynamical Systems in Neuroscience* (MIT, Cambridge, MA).
45. Wilson CJ, Beverlin B, 2nd, Netoff T (2011) Chaotic desynchronization as the therapeutic mechanism of deep brain stimulation. *Front Syst Neurosci* 5:50.
46. Gras C, et al. (2002) A third vesicular glutamate transporter expressed by cholinergic and serotoninergic neurons. *J Neurosci* 22:5442–5451.
47. Beurrier C, Congar P, Bioulac B, Hammond C (1999) Subthalamic nucleus neurons switch from single-spike activity to burst-firing mode. *J Neurosci* 19:599–609.
48. Jiao Y, et al. (2000) Identification of the anterior nucleus of the ansa lenticularis in birds as the homolog of the mammalian subthalamic nucleus. *J Neurosci* 20:6998–7010.
49. Goldberg JH, Fee MS (2012) A cortical motor nucleus drives the basal ganglia-recipient thalamus in singing birds. *Nat Neurosci* 15:620–627.
50. Person AL, Perkel DJ (2005) Unitary IPSPs drive precise thalamic spiking in a circuit required for learning. *Neuron* 46:129–140.
51. Person AL, Perkel DJ (2007) Pallidal neuron activity increases during sensory relay through thalamus in a songbird circuit essential for learning. *J Neurosci* 27:8687–8698.
52. Boulland J-L, et al. (2009) Vesicular glutamate and GABA transporters sort to distinct sets of vesicles in a population of presynaptic terminals. *Cereb Cortex* 19:241–248.
53. Fattorini G, et al. (2009) VGLUT1 and VGAT are sorted to the same population of synaptic vesicles in subsets of cortical axon terminals. *J Neurochem* 110:1538–1546.
54. Kao Y-H, et al. (2004) Evidence that certain retinal bipolar cells use both glutamate and GABA. *J Comp Neurol* 478:207–218.
55. Root DH, et al. (2014) Single rodent mesohabenular axons release glutamate and GABA. *Nat Neurosci* 17:1543–1551.
56. Shabel SJ, Proulx CD, Piriz J, Malinow R (2014) Mood regulation. GABA/glutamate co-release controls habenula output and is modified by antidepressant treatment. *Science* 345:1494–1498.
57. Zander J-F, et al. (2010) Synaptic and vesicular coexistence of VGLUT and VGAT in selected excitatory and inhibitory synapses. *J Neurosci* 30:7634–7645.
58. Aronov D, Veit L, Goldberg JH, Fee MS (2011) Two distinct modes of forebrain circuit dynamics underlie temporal patterning in the vocalizations of young songbirds. *J Neurosci* 31:16353–16368.
59. Goldberg JH, Fee MS (2011) Vocal babbling in songbirds requires the basal ganglia-recipient motor thalamus but not the basal ganglia. *J Neurophysiol* 105:2729–2739.
60. Kojima S, Kao MH, Doupe AJ (2013) Task-related "cortical" bursting depends critically on basal ganglia input and is linked to vocal plasticity. *Proc Natl Acad Sci USA* 110: 4756–4761.
61. Leblois A, Bodor AL, Person AL, Perkel DJ (2009) Millisecond timescale disinhibition mediates fast information transmission through an avian basal ganglia loop. *J Neurosci* 29:15420–15433.
62. Boettiger CA, Doupe AJ (1998) Intrinsic and thalamic excitatory inputs onto songbird LMAN neurons differ in their pharmacological and temporal properties. *J Neurophysiol* 79:2615–2628.
63. Bottjer SW, Brady JD, Walsh JP (1998) Intrinsic and synaptic properties of neurons in the vocal-control nucleus IMAN from in vitro slice preparations of juvenile and adult zebra finches. *J Neurobiol* 37:642–658.
64. Bottjer SW (2005) Silent synapses in a thalamo-cortical circuit necessary for song learning in zebra finches. *J Neurophysiol* 94:3698–3707.
65. Johnson F, Sablan MM, Bottjer SW (1995) Topographic organization of a forebrain pathway involved with vocal learning in zebra finches. *J Comp Neurol* 358:260–278.
66. Luo M, Ding L, Perkel DJ (2001) An avian basal ganglia pathway essential for vocal learning forms a closed topographic loop. *J Neurosci* 21:6836–6845.
67. Vates GE, Nottebohm F (1995) Feedback circuitry within a song-learning pathway. *Proc Natl Acad Sci USA* 92:5139–5143.
68. Rajan K, Abbott LF, Sompolinsky H (2010) Stimulus-dependent suppression of chaos in recurrent neural networks. *Phys Rev E Stat Nonlin Soft Matter Phys* 82:011903.
69. Kimpo RR, Theunissen FE, Doupe AJ (2003) Propagation of correlated activity through multiple stages of a neural circuit. *J Neurosci* 23:5750–5761.
70. Hoffmann LA, Saravanan V, Wood AN, He L, Sober SJ (2016) Dopaminergic contributions to vocal learning. *J Neurosci* 36:2176–2189.
71. Friend DM, Kravitz AV (2014) Working together: Basal ganglia pathways in action selection. *Trends Neurosci* 37:301–303.
72. Boulland J-L, et al. (2004) Expression of the vesicular glutamate transporters during development indicates the widespread corelease of multiple neurotransmitters. *J Comp Neurol* 480(3):264–280.
73. Gillespie DC, Kim G, Kandler K (2005) Inhibitory synapses in the developing auditory system are glutamatergic. *Nat Neurosci* 8(3):332–338.
74. Goldberg JH, Adler A, Bergman H, Fee MS (2010) Singing-related neural activity distinguishes two putative pallidal cell types in the songbird basal ganglia: Comparison to the primate internal and external pallidal segments. *J Neurosci* 30(20):7088.
75. National Research Council (2011) *Guide for the Care and Use of Laboratory Animals* (National Academies Press, Washington, DC), 8th Ed.